Journal of Applied Fluid Mechanics, Vol. 10, No. 1, pp. 95-102, 2017.
Available online at www.jafmonline.net, ISSN 1735-3572, EISSN 1735-3645.
DOI: 10.18869/acadpub.jafm.73.238.26678

Experimental Investigation on Supercavitating Flow over Parabolic Cavitators

M. Moghimi†, N. M. Nouri and E. Molavi

Mechanical Engineering Department, Iran University of Science and Technology, Tehran, 3114-16846, Iran

†*Corresponding Author Email: moghimi@iust.ac.ir*

(Received June 12, 2016; accepted July 30, 2016)

ABSTRACT

In this paper experimental study was carried out to investigate supercavitation around parabolic cavitators. Various types of cavitators, such as disk, cone, and parabolic, were designed and manufactured. Also, the shape of the cavities formed behind these bodies were considered and compared. Dimensionless parameters such as dimensionless length and the diameter of the cavity as well as the dimensionless required air flow on the cavitators were obtained. The results showed that parabolic cavitators have an optimum design in comparison with the disk and cone cavitators due to their insignificant capability to reduce the drag force, yet the cavity's length has a moderate size. It was also observed that this type of cavitator is capable of forming a cavity with a dimensionless length up to L/d= 33 and a dimensionless width up to D/d= 3.6. Moreover, parabolic cavitators require the highest amount of air injected in comparison with the cone and disk types; therefore, they operate in lower cavitation numbers. Since no other experimental data has been reported so far, this work reports the experimental characteristic behavior of parabolic cavitators.

Keywords: Supercavitation; Cavitation; Parabolic cavitator; Drag reduction.

NOMENCLATURE

$b_{1..2}$	length parameter
C_q	non-dimensional air flow rate
d	cavitator diameter
D	cavity Diameter
L	cavity length
Pc	cavity pressure
P∞	upstream pressure
Q	air flow rate
U∞	upstream velocity
$X_{1..3}$	coordinate points
ρ	density
η	parameter
σ	cavitation number
$\omega_{1..3}$	weight function variable

1. INTRODUCTION

Supercavitation is a hydrodynamic phenomenon in which a bubble cavity envelopes a submerged moving body. Supercavitation is a stage of cavitation in which the ratio of static to dynamic pressure of liquid flow is very small; i.e. between 0.3 and 0. Thus, instead of some cavitation bubbles on the solid surface, there will be a single huge cavity which envelops the whole body, Nouri *et al*. (2009). Regarding this situation, since the surface of the body is not in contact with water and the viscosity of vapor is much lower than that of water, the exerted drag force to the object decreases significantly. If the entire body is immersed in cavity, the friction drag can be reduced significantly by 90%, Ceccio (2010).

Supercavitation essentially occurs where the cavitation number has very low values. There are three different ways to achieve this situation: (1) increasing the speed of the moving object to very high values, i.e. natural supercavitation; (2) decreasing the ambient pressure (only possible in closed-circuit water tunnels); and (3) increasing the cavity pressure by ventilating air into the cavity, i.e. ventilated or artificial supercavitation.

The total drag force consists of viscous part and the pressure part. In supercavitation regime the viscous drag part decreases because of shear stress reduction near the submerged vehicle walls while the pressure drag part increases. However the total drag force decreases significantly. In recent years, supercavitation has received great attention by

researchers due to its capability of reducing the skin friction drag and enabling the submerged vehicle to travel at very high speeds. The submereged vehicle has four main parts including node, midbody, tail and control surfaces which has individual participation in total drag force. One of the most important parts of the body is the shape of the nose or cavitator, which causes the creation of the cavity to engulf the whole body. A large number of studies have been conducted to investigate the effect of cavitator shape on supercavitation and flow characteristics. One of the pioneers in the field of supercavitating flows is Reichardt (1969), who studied the axi-symmetric supercavitating flows experimentally. He also showed the possibility of creation of artificial supercavitation by means of gas ventilation around a body. Rouse and McNown (1948) carried out a series of experiments on natural cavitation around axi-symmetric configurations. The cavitators were in the form of hemispherical, conical, and ogival and blunt fore-body shapes. Waid (1957) measured the cavity shapes for flat plates and wedges.

Wei *et al.* (2007) investigated the effect of some similar parameters on the character of ventilated supercavity on the basis of experimental results. Their results showed that the Froude number, the dimensionless ventilated flow rate, and the natural cavitation number have more important effects on the character of the ventilated supercavity. The dimensionless ventilated flow rate is a determinant parameter, while the Froude number causes the shape of ventilated supercavity to be unsymmetrical.

Kawakami and Williams (2009) experimentally investigated the ventilated supercavitation formed behind a sharp-edged disk utilizing several different configurations. Zhang *et al.* (2009) designed three different front profiles for supercavitating vehicles based on the cavity theory as well as the Granville streamlined Equation and tested them in a high-speed water tunnel. Their experimental results showed that the front profile of a supercavitating vehicle affects the supercavity generation speed and the critical gas flow rates. The smaller the changes in the axial distribution of pressure, the higher the supercavity generation speed. Numerical studies were also conducted on the cavitation of different cavitators. Cavitation of disks in axisymmetric tunnels, Brennen (1969), disks in square-section tunnels, Street (1977), and cones in axisymmetric tunnels, Amormin and Ivanov (1976), are some instances of such studies. Xiang *et al.* (2011) conducted a numerical study on ventilated supercavitation. Shafaghat *et al.* (2009) investigated the mathematical behavior of axisymmetric supercavitating flow parameters, including the drag coefficients of supercavitating cones and disks and the cavitation number and maximum cavity width for a wide range of cone and disk diameters, cone tip angles, and cavity lengths. For this reason, they first developed a CFD code based on a direct boundary element method. After verifying the code, they used the data from the software to propose appropriate mathematical functions describing the behavior of these parameters. They showed that, among all available functions such as linear, polynomial, logarithmic, power, and exponential, only power functions can very well describe the behavior of the mentioned parameters. Shafaghat *et al.* (2008) studied the shape optimization of two-dimensional cavitators in supercavitating flows. They used the so-called Non-dominated Sorting Genetic Algorithm NSGAII) to optimize cavitator shapes in supercavitating flows. In another study, Shafaghat *et al.* (2011) identified parabolic cavitators as the optimum cavitators for drag reduction. Pendar and Roohi (2016) is also numerically studied the cavity characteristics for the head-form body and conical cavitators under different cavitation and turbulence models. Mostafa (2016) used bubble dynamics cavitation to simulate cavity over a hydrofoil under different cavitation numbers and angle of attacks.

In this study, the supercavitation of parabolic cavitators has been experimentally investigated. Moreover, the cavitation of different types of cavitators was also tested and compared with parabolic cavitators. In order to investigate the effect of cavitator shape on the aspects and properties of the cavity, the tests have been carried out in a high speed water tunnel at the applied hydrodynamics laboratory of the Iran University of Science & Technology (IUST). Three various kinds of cavitators were designed, including three cones with vertex angles of 45, 60, and 90 degrees, two parabolic cavitators with different curvature radiuses, and one disk. This paper focuses on some important aspects of the cavity, such as dimensionless length and diameter of the cavity for parabolic cavitators. These aspects have been measured at various flow conditions and different cavitation numbers. Finally, diagrams of the mentioned supercavity properties versus the cavitation number are drawn for all of these cavitators, and the effects of flow conditions on the properties and shapes of the supercavity are investigated. This study is unique in terms of its experimental investigation of the behavior of parabolic cavitators, which has not been reported so far.

2. EXPERIMENTAL STUDY

2.1. Experimental Setup

The experiments were carried out in a high speed water tunnel at the applied hydrodynamics laboratory at IUST. This tunnel has four test sections, with a cross section area of 10×20 cm2 and a length of 84 cm. The water pump drives the water with a maximum velocity of 8 m/s in the water tunnel. Since this velocity was not sufficient to decrease the cavitation number and form a supercavity, the absolute pressure of the tunnel was reduced and air was injected into the cavity to achieve an artificial supercavitation. Two vacuum pumps in the series are capable of decreasing the total pressure of the tunnels to a value as low as 0.2 bars. The closed-circuit water tunnel is depicted in Fig. 1. As shown in Fig. 2, the cavitators were designed in such a manner that they would be mounted on the strut inside the water tunnel. For that reason, the cavitators have a threaded hole for

screwing onto the strut. To inject the air into the cavity, some holes were created on the conic part of the strut top, as seen in Fig. 3. An orifice is used to measure the flow rate of the ventilated air and also 11 pressure transducers, Honeywell models 142 PC 15A, 163 PC 01 D75, and 164 PC 01 D76 were used in order to measure the pressure at different points of the tunnel. The water flow rate is measured by means of an electromagnetic flow meter, Endress+Hauser Flowtec model Proline Promag 10 P, in the test section. All data were recorded in PC real time, and the obtained data were processed offline. The schematic presentation of the water tunnel to create a ventilated supercavity is shown in Fig. 2.

Fig. 1. Closed-circuit water tunnel.

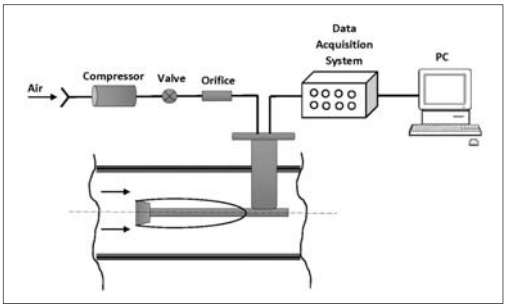

Fig. 2. Schematic presentation of the apparatus used to create ventilated supercavity.

Fig. 3. Cavitator mounted on strut and the nozzles used for air injection.

2.2. Cavitators

Three types of cavitators were designed and manufactured in order to investigate the geometrical features of the cavity behind each of them. The disk cavitator diameter is 10 mm. The other cavitator is the conical one with vertex angles of 45, 60, and 90 degrees. The specifications of these cavitators are shown in Fig. 4. The cavitator shape affects the cavity size as well as the amount of exerted drag force. Shafaghat *et al.* (2008) investigated the optimum shape of the cavitators for minimum drag force and identified the parabolic geometries. Parabolic cavitators have an optimized shape, between flat (disk) and conical cavitators with regard to the drag force reduction. They claimed that these cavitators have better capabilities than the disk and conical cavitators (Shafaghat, 2011). As such, parabolic cavitators were tested experimentally in water tunnel. Two parabolic cavitatiors with two different curvature radiuses, i.e. types I and II, were designed.

The profile of the parabolic cavitators was extracted from Eq. (1) (Shafaghat, 2008):

$$X_\eta = \frac{(1-\eta^2)X_1\omega_1+2\eta(1-\eta)X_2\omega_2+\eta^2X_3\omega_3}{(1-\eta)^2\omega_1+2\eta(1-\eta)\omega_2+\eta^2\omega_3} \quad (1)$$

where $X_1 = (-b_1, 0)$, $X_2 = (-b_1, b_2)$, $X_3 = (0,1)$, $\omega_1 = 1$ and $\omega_3 = 1$. X_1, X_2 and X_3 are the profile control points and $\omega_1$to ω_3 are the weight functions of points. Parameters b_1 and b_2 are design parameters. Parameter ω_2 is the weight value for the second point, X_2. The profile approaches the point X_2 as ω_2 becomes larger, whereas the profile is changed to a straight line, which connects point X_1 to X_3, as ω_2 becomes smaller and reaches zero (Fig. 5).

Therefore, the geometry of each cavitator is determined through three parameters, i.e. b_1,b_2, and ω_2. The specifications of the parabolic cavitators, i.e. types I and II, are given in Table 1.

Table 1 Specifications of manufactured parabolic cavitators

Type	b1	b2	□2	d (mm)
1	0.42	0.66	1.98	11.2
2	0.36	0.77	1.63	17.5

2.3. Experimental Procedures

Different regimes of cavitation can be produced in the water tunnel by changing the cavitation number. The cavitation number is defined as (Ceccio, 2010):

$$\sigma = \frac{P_\infty - P_c}{0.5\rho U_\infty^2} \quad (2)$$

where P_∞ and U_∞ are free stream pressure and velocity, respectively, ρ is the water density, and P_c is the cavity pressure. In order to achieve various cavitation numbers, the velocity of the water in the tunnel was changed through adjusting the valve which is located after the pump. It should be noted that, while the pressure of the tunnel was held constant, the cavity pressure was altered through injecting the air. The specifications of cavities including length, diameter, and the amount of air injected into the cavity were measured at specific cavitation numbers for different cavitators.

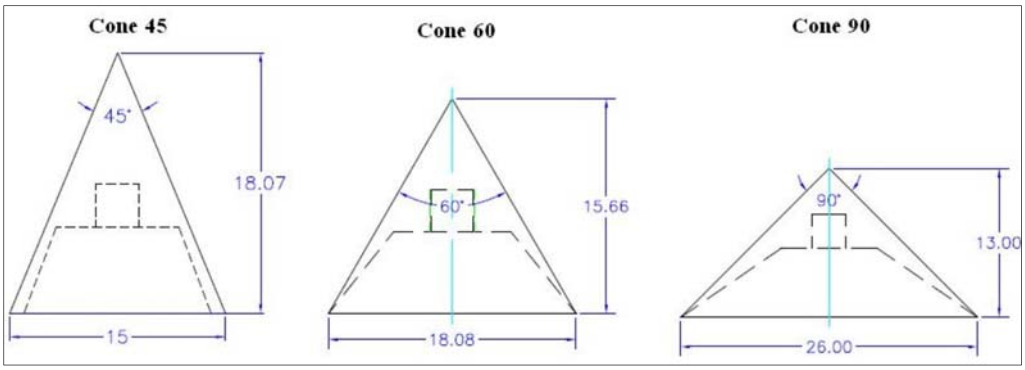

Fig. 4. Specifications of cone cavitators.

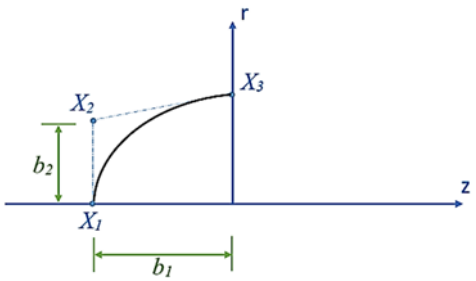

Fig. 5. Profile of the parabolic cavitators.

3. RESULTS AND DISCUSSIONS

Non-dimensional cavity length and width and the ventilated air flow rate are measured for different cavitation numbers and various cavitators. The geometrical parameters are depicted in Fig. 6.

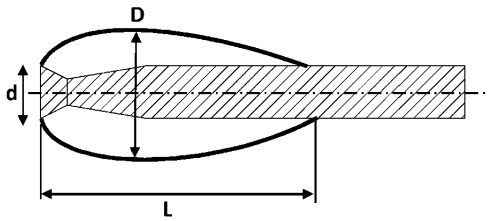

Fig. 6. Schematic of cavity closure and the geometrical parameters.

3.1. Cone Cavitators

Figures 7 and 8 show the supercavitation formed behind the cone cavitator with vertex angles of 45 and 60 degrees.

Fig. 7. Cavity behind the cavitator with a cone of 45°.

The cavity has a length of approximately 350 mm and a width of 36 mm. The cavity has an axi-symmetric shape except its end, i.e., the closure region. The Froud number based on the cavities diameter is 10, and the cavitation number is 0.18. It can be observed that the end of the cavity has moved upwards due to gravity forces and the difference in water and air densities. The Reynolds number of the flow inside the tunnel test section is about 2×10^6. Moreover, Fig. 8 shows that the cavity formed behind a cone with a vertex angle of 60°. In Figs. 9 and 10, the non-dimensional length and diameter of different cone cavitators are presented. It can be seen that, for the cone cavitator with a vertex angle of 45°, the non-dimensional length of the cavity could have values from 5 to 25 times larger than the cavitator diameter. Also, upon decreasing the cavitation number, the length and diameter of the cavity increase.

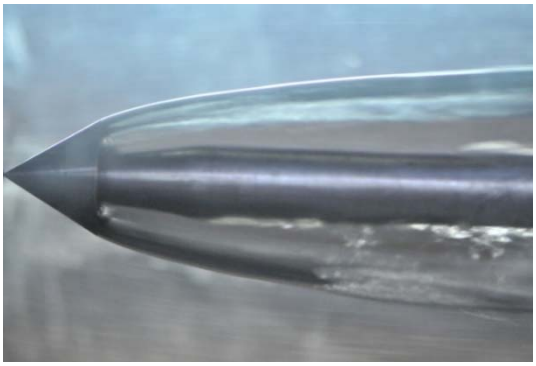

Fig. 8. Cavity behind the cavitator with a cone of 60° (cavitation number is 0.24).

Cone cavitators with larger vertex angles work at higher cavitation numbers than do cavitators with small vertex angles. Cone cavitators create cavities with short lengths and diameters; an increase in vertex angle will create longer cavities. It can also be concluded from Figs. 9 and 10 that the slope of the curve which is fitted to the experimental data grows as the vertex angle decreases. In other words, for a constant cavitation number, the cavity created behind the cone with larger vertex angle is longer and thicker.

For cone cavitators used in this study, L/d changes from 3 to 25, and D/d varies between 1.5 and 2.5; the largest cavities have been formed at a cavitation number of 0.146.

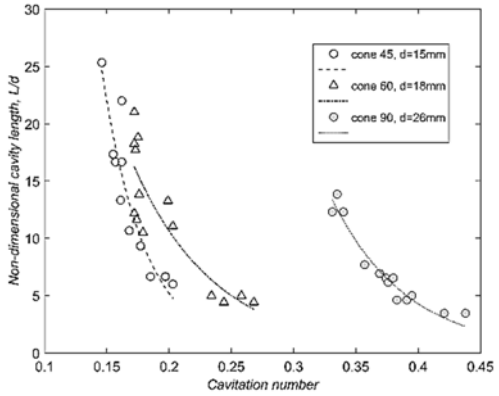

Fig. 9. Dimensionless cavity length for cone cavitators.

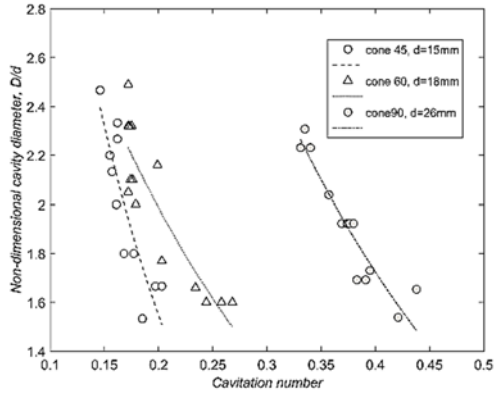

Fig. 10. Dimensionless cavity diameter for cone cavitators.

It can be seen that, for all of the cone cavitators, a decrease in cavitation number increases the supercavity length. This can also be seen in Fig. 11, which shows the real pictures of the cavity formed behind the conical cavitator.

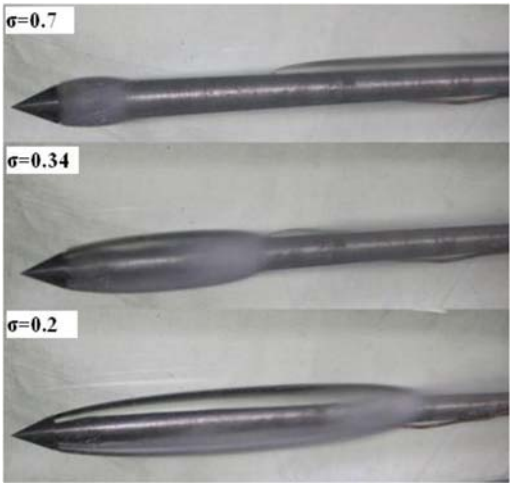

Fig. 11. Cavity growth by decreasing cavitation number.

3.2. Disk Cavitator

The supercavity formed behind the disk cavitator can be observed in Fig. 12. Figures 13 and 14 represent the non-dimensional length and diameter of cavity for a disk cavitator with different cavitation numbers. The most important point is that the cavity size growth rate, caused by a decrease in cavitation number, is very high; e.g. by decreasing the cavitation number from 0.22 to 0.14, the non-dimensional length of cavity increases from 5 d to 40 d.

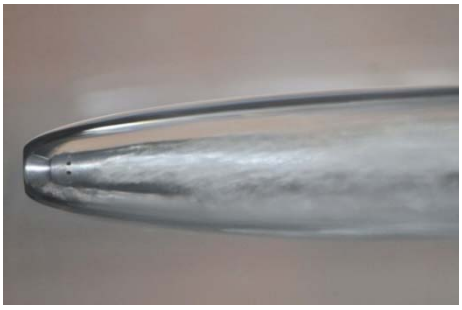

Fig. 12. Supercavity behind disk cavitator (cavitation number is 0.18).

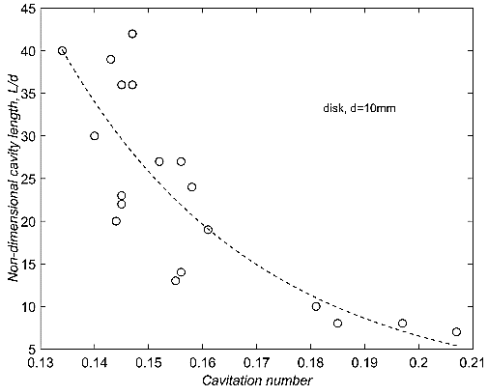

Fig. 13. Non-dimensional cavity length for disk cavitator.

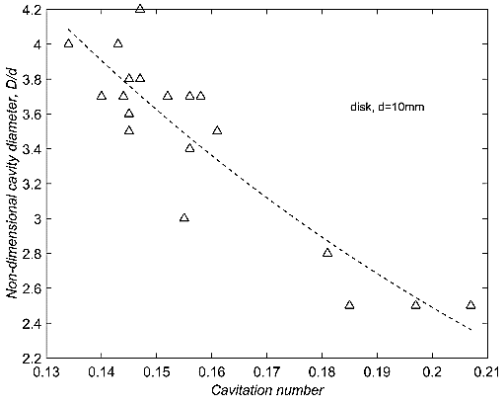

Fig. 14. Non-dimensional cavity diameter for disk cavitator.

3.3. Parabolic Cavitator

The optimum design of a parabolic cavitator was investigated by Shafaghat *et al.* (2011). The aim of

their optimization was to achieve minimum hydrodynamic drag force regarding the cavity shape. They used the boundary element method for this purpose and identified the optimum shape for the parabolic profile. In this study, the optimum shape (i.e. parabolic profile) was employed, and cavitators were manufactured and tested. The parabolic cavitator and the cavity profiles are depicted in Fig. 15. Cavitation number is 0.2 in this case.

Fig. 15. Cavity formed behind parabolic type 1 cavitator.

The cavity non-dimensional length and diameter for the parabolic cavitators are presented in Figs. 16 and 17. It can be seen that parabolic cavitators with larger diameters cover larger cavitation numbers. On the other hand, obtaining a specific cavity size with a smaller parabolic cavitator requires lower cavitation numbers.

The maximum L/d and D/d for parabolic cavitators are 32.14 and 3.57, respectively, and have occurred at a cavitation number of 0.07.

For better comparison, the obtained data of disk and parabolic cavitators are plotted in Figs. 18 and 19. The results show that the disk cavitator creates a much bigger cavity than the cone and parabolic cavitators. It can be observed that, as the cavitation number decreases, the non-dimensional length and diameter of the disk cavitator becomes much greater than those for the other cavitators. Since the drag force exerted on the cavitator decreases with reducing the cavitation number, there would be limitations in drag reduction by disk cavitaors. Due to their good dispersion (expansion) effect, cavities formed behind the disk cavitators are longer and wider in comparison to other cavitators, while at low cavitation numbers, cavity length has smoother variations for parabolic cavitators in comparison to that for the disk cavitators.

It should be noted that, in order to form supercavitation in larger cavitators, higher amounts of air are required; therefore, in this research, testing in the range of relatively high non-dimensional lengths was impossible in some cases. Generally speaking, the length of cavities increases with the decrease in the cavitation number for all types of the cavitators.

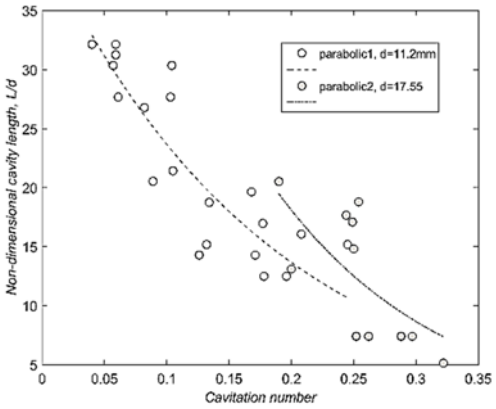

Fig. 16. Non-dimensional length of cavity for parabolic cavitators.

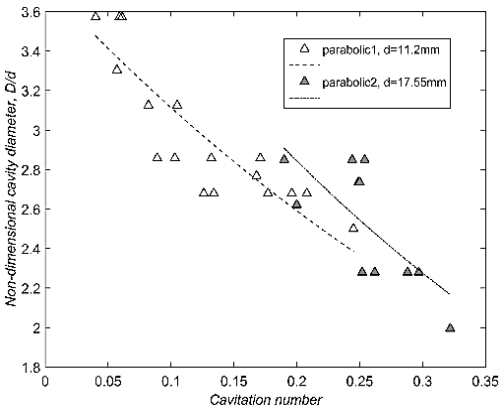

Fig. 17. Non-dimensional diameter of cavity for parabolic cavitators.

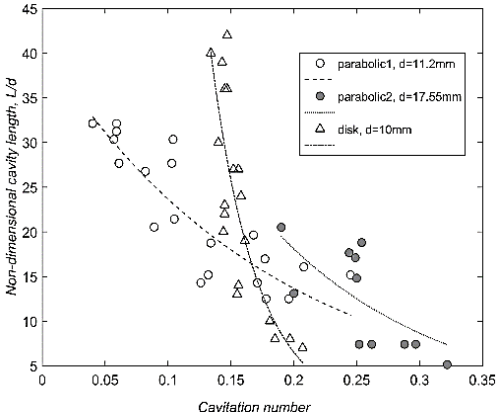

Fig. 18. Non-dimensional length of cavity for parabolic and disk cavitators.

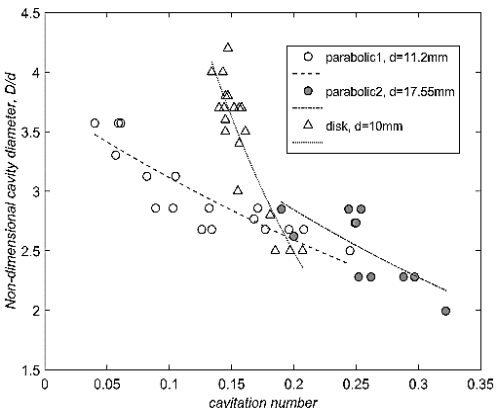

Fig. 19. Non-dimensional diameter of cavity for parabolic and disk cavitators.

3.4. Required Air for Ventilated Supercavitation

As mentioned earlier, due to the operational difficulties in achieving high speeds in water tunnels, artificial supercavitation, e.g. ventilated supercavitation, was studied. The required air, to maintain a supercavity of the given dimensions, varies for different cavitators. For this reason, the amount of injected air required to sustain an artificial cavity at different velocities was investigated. Throughout the experiments, the air flow rate injected into the cavity was measured by means of an orifice. For better comparison, the air flow rate is formulated in non-dimensional form as:

$$C_q = \frac{Q}{U_\infty \times d^2} \tag{3}$$

where U, Q, and d are flow velocity, air flow rate, and cavitator diameter, respectively. The non-dimensional air flow rates required for various cavitators are plotted in Fig. 20.

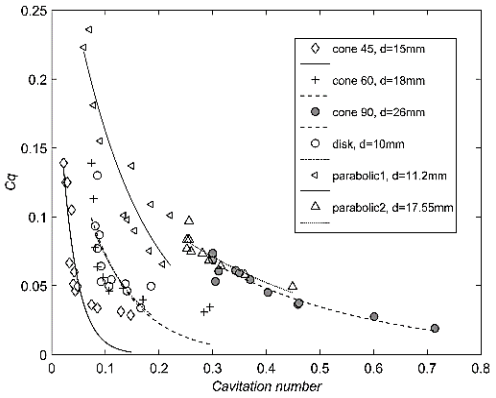

Fig. 20. Non-dimensional air flow rate.

As can be seen in Fig. 20, at low cavitation numbers, the required air for supercavitation increases. By injecting further amounts of air, the length of the cavity becomes longer and the stability of the cavity increases. It is obvious that shorter cavities, which correspond to higher cavitation numbers, require lesser amounts of air. Test results show that, for a specific cavitation number, by increasing the cone vertex angle, the amount of air required for forming supercavitation increases.

Another interesting result is that a disk cavitator can be assumed as a cone with the vertex angle of 180 degrees and thus should have a behavior in line with the 90-degree cone cavitator. However, it was observed that this cavitator has a position between the 45 and 60 degrees cavitators. It was also observed that parabolic cavitators require more air than disk cavitators to form a supercavity.

In general, to achieve longer cavities, the optimum design tends from disk cavitators towards cone cavitators and to achieve thicker cavities, the disk cavitator is the best choice. In the mid ranges of cavity length and diameters, the optimum choice is the parabolic cavitator.

4. CONCLUSIONS

In order to compare the supercavitation behind different cavitators, experimental tests were carried out for three types of cavitators in a high-speed water tunnel. The focus was, however, on parabolic cavitators, because no other experimental investigation has been reported in that field. Cone cavitators with low vertex angles have low drag but do not create a desirable cavity which could engulf the moving object. On the other hand, disk cavitators create large cavities, but they are not effective in reducing the drag forces. Parabolic cavitators can take advantage of both of these cavitators due to their design, which is something between cone and disk cavitators. Parabolic cavitators can form a cavity which has a proper size and could envelope the submerged body. At the same time, it can substantially reduce the drag force. Parabolic cavitators can be designed for different applications and can perform in different ways. They can also develop various capabilities by changing the design constants in their geometry. Some other remarkable conclusions were as follows:

1. The largest dimensionless supercavity size belongs to the supercavity formed behind the disk cavitator with the size of L/d= 42 and D/d=4.2, corresponding to a cavitation number of 0.15.
2. The disk cavitator creates the biggest cavity both in length and diameter. However, since this cavitator requires a higher cavitation number than the parabolic cavitator (type 1) and the cone cavitator with a vertex angle of 45°, it has limitations in drag reduction.
3. The cone cavitator with a vertex angle of 45° produces the longest cavity among the cone cavitators with the size of L/d= 25 at σ= 0.15.
4. Parabolic cavitators have a very interesting behavior. These cavitators not only produce long and thick cavities, but also work in a wide range of cavitation numbers, especially at low values of cavitation numbers, which means a better drag reduction.
5. Although parabolic cavitator type 1 needs large amounts of air to operate at low values of cavitation numbers, parabolic cavitator type 2 acts similar to the cone cavitator with a vertex angle of 90°.

ACKNOWLEDGMENT

The Applied Hydrodynamics research lab at Iran University of Science and Technology (IUST) is highly acknowledged for its financial support during the course of this project.

REFERENCES

Amromin, E. L. and A. N. Ivanov (1976). Axisymmetric cavitation behind a body in water tunnels. *Fluid Dynamics* 11, 532–7.

Brennen, C. (1969). A numerical solution of axisymmetric cavity flows. *Journal of Fluid Mechanics* 37, 671–88.

Ceccio, S. L. (2010). Friction drag reduction of external flows with bubble and gas injection. *Annual Review Fluid Mechanics* 42, 183–203.

Kawakami, E. and M. Williams (2009). *Investigation of the behavior of ventilated supercavities*, CAV2009 – Paper No. 111, 1–4.

Mostafa, N., M. M. Karim and M. M. A. Sarkar (2016). Numerical prediction of unsteady behavior of cavitating flow on hydrofoils using bubble dynamics cavitation model. *Journal of Applied Fluid Mechanics* 9 (4), 1829-1837.

Nouri, N. M. and A. Eslamdoost (2009). An iterative scheme for two-dimensional supercavitating flow. *Ocean Eng*ineering *Journal* 36, 708–15.

Nouri, N. M., M. Moghimi and S. M. Mirsaeedi (2009). Numerical simulation of unsteady cavitating flow over a disk. In *Proceedings of the Institution of Mechanical Engineers, Part C: Journal of Mechanical Engineering Science 224(6), 1245-1253.*

Pendar, M. R and E. Roohi (2016). Investigation of cavitation around 3D hemispherical head-form body and conical cavitators using different turbulence and cavitation models. *Ocean Engineering Journal* 112, 287-306

Reichardt, H. (1969). The law of cavitation bubbles at axially symmetric bodies in a flow. *Reports Translation Ministry Aircraft Production*, UK, 766.

Rouse, H. and J. McNown (1948). *Cavitation and pressure distribution: head forms at zero angle of yaw*. *State Univ Iowa: Bulletin*.

Shafaghat, R, S. M. Hosseinalipour, I. Lashgari and A. Vahedgermi (2011). Shape optimization of axisymmetric cavitators in supercavitating flows, using the NSGA II algorithm. *Applied Ocean Research* 33, 193–8.

Shafaghat, R., S. M. Hosseinalipour, N. M. Nouri and A. Vahedgermi (2009). Mathematical approach to investigate the behavior of the principal parameters in axisymmetric supercavitating flows, using boundary element method. *Journal of Mechanics* 25(4), 465–73.

Shafaghat, R., S. M. Hosseinalipour, N. M. Nouri and I. Lashgari (2008). Shape optimization of two-dimensional cavitators in supercavitating flows, using NSGA II algorithm. *Applied Ocean Research* 30, 305–10.

Street, R. L. (1977) A review of numerical methods for solution of three dimensional cavity problems. In *Proceeding of International conference on Numerical Ship Hydrodynamics,* 237–249.

Waid, R. L. (1957). Water tunnel investigation of two-dimensional cavities, Report *(California Institute of Technology. Hydrodynamics Laboratory)*, E-73.6.

Wei, Y. J., W. Cao, C. Wang, J. Z. Zhang and Z. Z. Zou (2007). Experimental Research on Character of Ventilated Supercavity. *Fifth Int. Conf. Fluid Mech., Shanghai, China*. 348–51.

Xiang, M., S. C. P. Cheung, J. Y. Tu and W. H. Zhang (2011). Numerical research on drag reduction by ventilated partial cavity based on two-fluid model. *Ocean Engineering Journal* 38(17), 2023-2032.

Zhang, B., Y. Zhang and X. Yuan (2009). Effects of the profile of a supercavitating vehicle's front-end on supercavity generation. *Journal of Marine Science and Application,* 8, 323–7.